Journal of the European Ceramic Society 22 (2002) 1381–1385

www.elsevier.com/locate/jeurceramsoc

Effect of microstructural evolution on the mechanical properties of lepidolite based glass-ceramics

Ping-An Fang*, Zhao-Ping Wu

State Key Lab of High Performance Ceramics and Supertine Microstructures, Shanghai Institute of Ceramics, Chinese Academy of Sciences, 1295 Dingxi Road, Shanghai 200050, China

Received 8 May 2001; received in revised form 6 August 2001; accepted 15 August 2001

Abstract

In this paper, effect of microstructural evolution on mechanical property of lepidolite based glass-ceramics of $MgO–Al_2O_3–SiO_2–Li_2O–R_2O–F(R = Na, K)$ system during the crystallization process has been studied. The results show that two distinct regions of strength dependence on grain size are found. The critical values of the flake diameter and aspect ratio of lepidolite are 1.8 and 4.6μm, respectively. The crystallization temperature (T_C) of critical point locates at 1060 °C. When $T_C \leqslant 1060$ °C, the bending strength increases with heat-treatment temperature ascribing to the randomly oriented and interlocked lepidolite crystallites, which cause crack divert or blunt to limit the further development of the flaw size and increase the surface energy of fracture. While $T_C >$ 1060 °C, the increased boundary shear stress arising from the mismatch of thermal coefficient between the lepidolite crystallite and the residual glass phase results in the decrease of strength.

Keywords: Glass–ceramics; Grain size; Lepidolite; Microstructure-final; Strength

1. Introduction

Mica-based glass-ceramics attract great interest since they were first reported by Grossman[1] due to their unique machinability resulting from the cleavage of interlocking layers of mica crystallites dispersed in a glassy matrix. The materials can be machined to precise tolerence with conventional metal working tools, thus solving a major parts-fabrication problem. The materials do not sacrifice strength, hardness or porosity to achieve this machinability, nor do they have to be fired after machining. Therefore they can be used in a wide field of applications, such as mechanical parts,[2] electrical insulators,[3] vacuum equipment,[4] dental crowns and bones.[5]

Up to now, three types of mica glass-ceramics with tetrasilicic mica ($KMg_{2.5}Si_4O_{10}F_2$),[3,6] fluorophlogopite mica($KMg_3AlSi_3O_{10}F_2$) [7–11] and barium(calcium) mica $[Ba(Ca)_{0.5}Mg_3AlSi_3O_{10}F_2]$[12–15] as main crystal phase respectively, have been intensively investigated. However, lepidolite based glass-ceramics with lepidolite and its solid solution $[K(Na)Li(Mg,Al)AlSi_3O_{10}F_2]$ as main crystal phase, have been rarely reported.[16,17] In addition to offering easy machinability, lepidolite based glass-ceramics[17] show good chemical durability, high thermal shock damage resistance and lower thermal coefficient ($< 50\times10^{-7}$ °C^{-1}) than other kinds of mica glass-ceramics ($> 60\times10^{-7}$ °C^{-1}) due to introduing Li_2O into glass matrix.

Generally, mica based glass-ceramics exhibit insufficient mechanical strength, so do lepidolite based glass–ceramics. The mechanical properties of glass-ceramics are highly dependent on their crystalline phase assemblages and microstructures. Many studies[2,11,14,15] showed that the mechanical properties of mica glass-ceramics are mainly influenced by mircostrutral varibles, such as morphology of precipitated mica, crystalline size, aspect ratio and crystallinity. In the present paper, the system of K_2O (Na_2O)–$MgO–Al_2O_3–SiO_2–Li_2O–F$ was used as a base glass composition, from which lepidolite glass-ceramics were obtained after heat treatment. The novel mechanical properties of lepidolite glass-ceramics have been found and studied in connection with their microstructural evolution.

2. Experimental procedures

The composition of the base glass in weight percent was SiO_2 55%, Al_2O_3 19%, MgO 9%, ($Na_2O + K_2O$) 7%,

* Corresponding author. Tel.: +86-021-62512990×6411; fax: +86-021- 62513903.

E-mail address: pinganfang@hotmail.com (P.-A. Fang).

0955-2219/02/$ - see front matter
PII: S0955-2219(01)00436-8

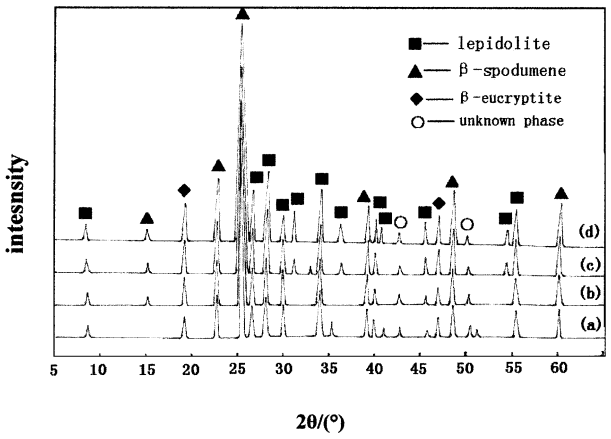

Fig. 1. XRD analysis of specimens at four different temperatures; (a) 950 °C, (b) 1000 °C, (c) 1060 °C, (d) 1120 °C.

Li_2O 3.9% and F 3%. To modify the microstructure and crystallinity, the base glass was doped with 3.1 wt.% ZrO_2 .The mixture was melted in a platinum crucible at 1480–1600 °C for 3 h, then the melt was poured onto an iron plate and casted into glass specimens. The resultant glass specimens annealed for 1 h near the glass transition temperature (500 °C) were given typical nucleation and crystallization treatments for 2 h at 650 °C and 8 h in the range of 950–1120 °C, respectively.

The presence of crystalline phases of crystallized specimens was identified by X-ray diffraction analysis (XRD, D/Max-Radiffractomer, Rigaku, Japan) with Cu K_α radiation. The specimens for microstructural observation were cut from the crystallized glass body. The surface morphologies of specimens, polished and chemically etched in HF acid (5 wt.%) at room tem-

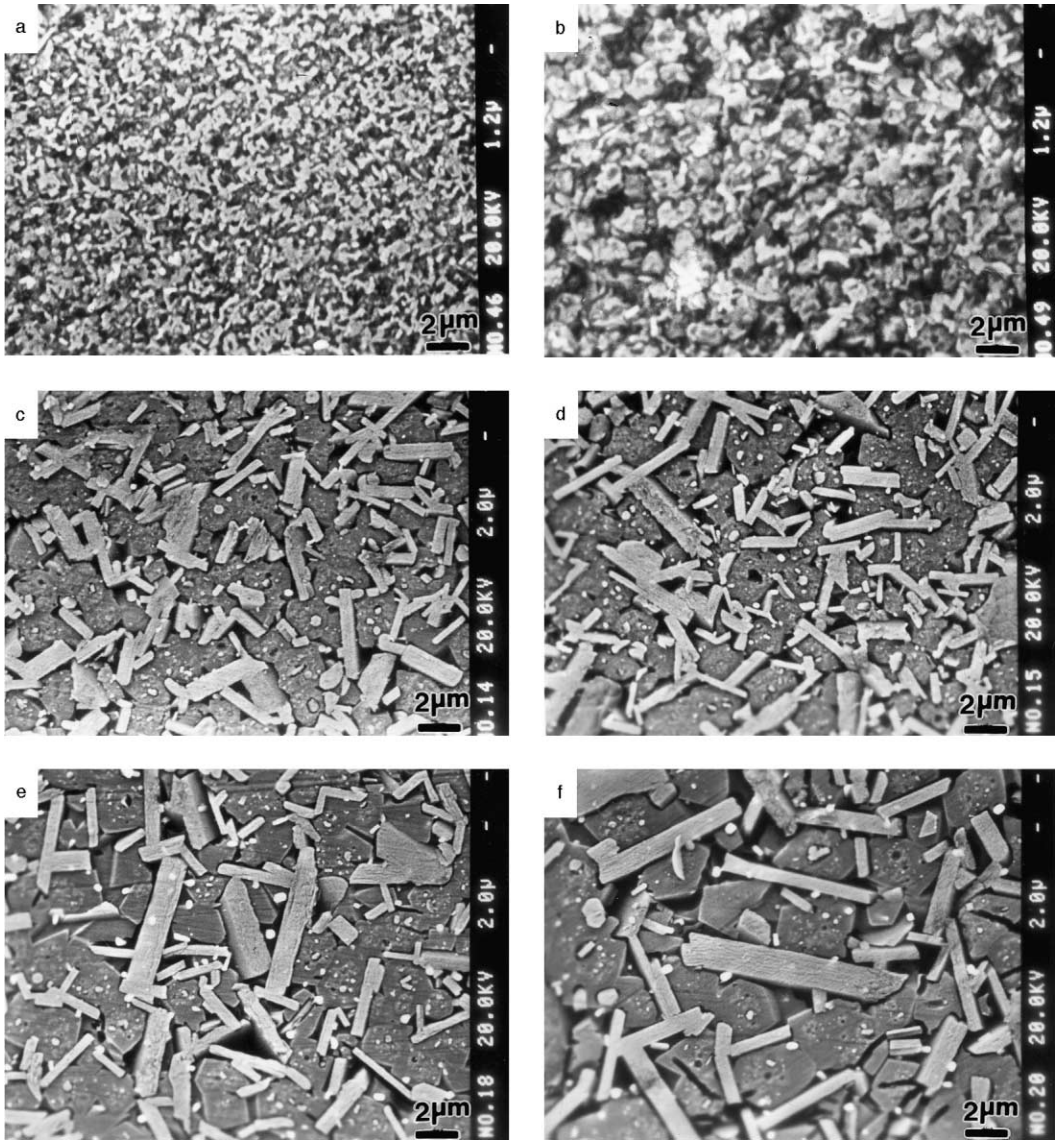

Fig. 2. SEM morphology of samples at various heat-treatment temperature; (a) 950 °C, (b) 1000 °C, (c) 1060 °C, (d) 1080 °C; (e) 1100 °C, (f) 1120 °C, all specimens were etched by HF (5%) for 30 s.

perature for 30 s, were examined with Scanning Electron Microscope (SEM, EPMA-8705QHZ, Shimadzu, Japan). To estimate the size and aspect ratio of crystals, a group of 15 crystals were selected in SEM photo of each specimen. The length and the thickness of cross section of each crystal were measured. The crystal size was calculated by averaging the lengths over the group. Dividing the length by the thickness of each crystal and averaging the results over the group, the aspect ratio was obtained. The error of measurment was estimated to be less than 5%.

The bending strength was measured for all the specimens by an Instron (1195) Universal Testing Machine in three-point bending in air with an internal spanning of 40mm and a crosshead speed of 0.5 mm/min at room temperature. At least 8 pieces were tested for each data point. The dimensions of tested pieces were $5\times5\times50$ mm.

3. Results and discussion

Fig. 1 shows XRD patterns of the crystallized glasses. After the crystallization stage in the range of 950–1120 °C for 8 h, two main crystalline phases, lepidolite (including its solid solution) and β-spondumene respectively, were detected in all specimens besides minor β-eucryptite and some unknown phase. In the series of heat treatment from 950 to 1120 °C, the X-ray diffraction lines become progressively sharper and more distinct as the heat-treatment temperature increased. They indicate that all specimens have the same crystalline phase and crystallinity increases with the increasing heat-treatment temperature.

Fig. 2 shows microstructural evolution of crystallized specimens from 950 to 1120 °C. At 950 °C, many interlocking crystals smaller than 0.6 μm were precipitated (Fig. 2a); fine equiaxed lepidolite crystals appeared at 1000 °C and the cross section of crystal exhibits cleavage structure (Fig. 2b). As the temperature is further increased above 1060 °C, the lepidolites grow up rapidly and assume a more elongated platelike appearance (Fig. 2 c, d, e, f) .The size and aspect ratio of lepidolite measured in photos are presented in Table 1. The results show that the size of lepidolite grow up more quickly above 1060 °C than below 1060 °C similar to change in morphology. Here we think, above 1060 °C, some amount of β-spondumenes are transformed into lepidolite and its solid solution incongruently with Mg^{2+}, K^+, Na^+ and F^- diffusing into it due to the reaction (1) between β-spondumene and glass matrix by metasomatism, which results in increase of lepidolite.

$$\mathrm{Li(AlSi_2O_6)} \xrightarrow{\mathrm{Mg^{2+},\ K^+,\ Na^+,\ F^-}} \mathrm{K(Na)Li(Mg,\ Al)Al\ Si_3\ O_{10}F_2} \quad (1)$$

Table 1
Size of lepidolite crystal at various heat-treatment temperature

Temperature /°C	950	1000	1060	1080	1100	1120
Average diameter /μm	0.58	0.90	1.76	2.87	4.09	5.15
Average thickness /μm	0.20	0.24	0.38	0.53	0.56	0.60
Aspect ratio	2.90	3.75	4.63	5.42	7.32	8.52

Fig 3.(a) shows measured data of the bending strength of all the specimens with change in size of lepidolite in the rang of 950–1120 °C, and the relationship between bending strength and aspect ratio is shown in Fig. 3(b). The results exhibit that, two distinct regions of strength dependence on grain size are found. When the flake diameter is small ($\leqslant$1.8μm) and the aspect ratio is small ($\leqslant$4.6), the bending strength increases with increasing grain size and aspect ratio; while the flake diameter and aspect ratio exceed the critical values, which are 1.8 and 4.6 μm, respectively, the bending strength decreases. The heat-treatment temperature of critical point locates at 1060 °C. It is similar to the results of tetrasilicic mica glass-ceramics reported by Grossman,[1] but it is not linear relationship between the bending strength and grain size or aspect ratio.

Characteristic microstructures of mica glass ceramics consist of uniformly distributed two dimensional mica crystals of random orientation in a brittle glass matrix.

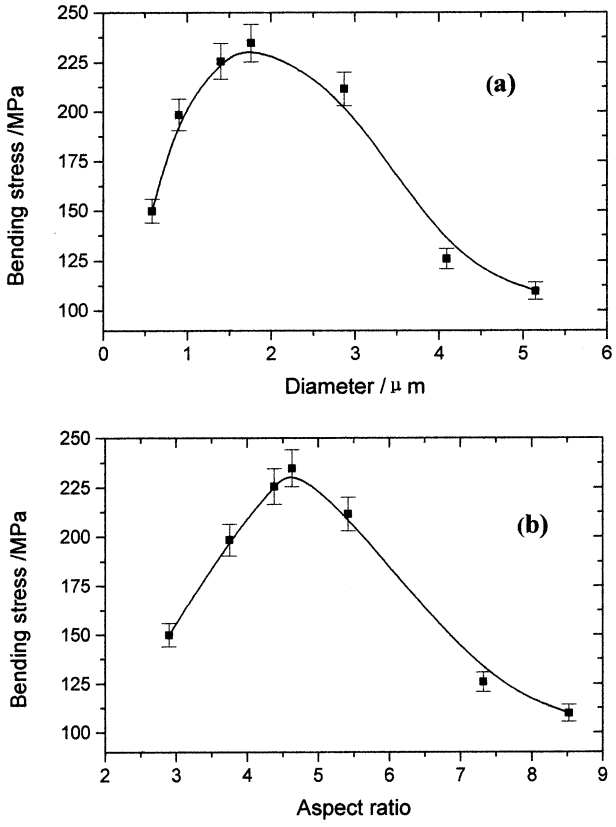

Fig. 3. Relationship between bending strength and size of lepidolite crystal; (a) σ—diameter, (b) σ—aspect ratio.

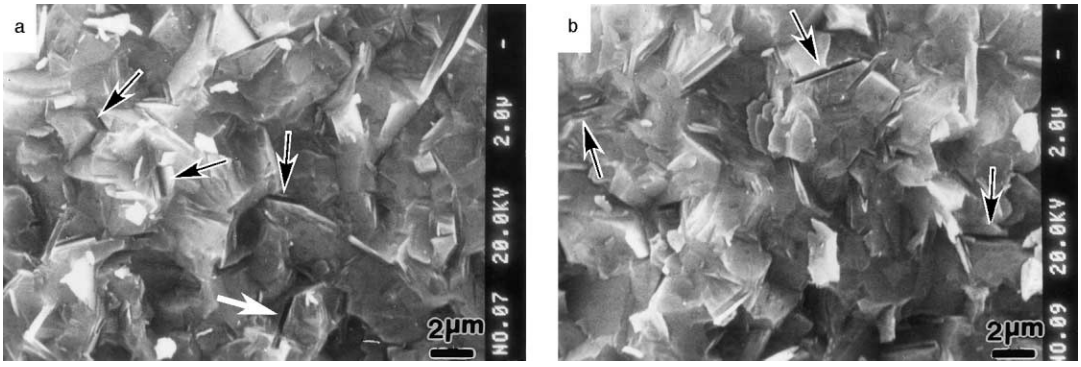

Fig. 4. Two types of morphology of specimens cross section at two different heat-treatment temperatures; (a) 1060 °C, (b) 1100 °C.

Therefore, the cracks are expected to nucleate at these preferred sites since a thermal expansion mismatch between the glass and the anisotropic mica crystals is unavoidable. When $T_C \leqslant 1060$ °C, as the lepidolite crystals become larger, randomly oriented and interlocking lepidolite crystals cause cracks to divert or deflect away from the initial planar path perpendicular to the tensile axis. Crack deflection become more effective in limiting the flaw sizes within the materials, which increase the absorption of energy released upon crack propagation. Such energy-absorbing fracture propagation must increase the effective surface energy of fracture. When the absorption of energy is great enough, crack can be blunted (denoted by arrow in Fig. 4a) and its fracture mode appear to be mainly intergranular, thus strength increases. While the flake diameter and aspect ratio exceed the critical values, where heat treatment temperature is above 1060 °C, the bending strength decrease can be due to shear stresses arising from the difference in the thermal expansion coefficients between the mica crystals and the residual glass phase. The boundary shear stresses play a marked role in the nucleation of larger crack (shown by arrow in Fig. 4b) at the boundary because of many mismatches between the mica crystals and the residual glass phase as crystals size get much longer.The coefficients of thermal expansion vary considerably over the range of solid solution in mica along a-, b-, c-axis. This strong anisotropy in thermal expanion makes it impossible to totally eliminate the internal stresses in mica glass-ceramics. When the boundary shear stresses development becomes so greater that the strengthening resulting from particles elongation can be ignored, then the strength decreases.

4. Conlusions

Lepidolite based glass-ceramics were formed from $MgO\text{-}Al_2O_3\text{–}SiO_2\text{–}Li_2O\text{–}R_2O\text{–}F(R = Na, K)$ system. The lepidolite can be recrystallized and grows up in the range of 950–1120 °C during the crystallization process. Effect of microstructural evolution on mechanical property was also investigated. The results show that, two distinct regions of strength dependence on grain size are found. The critical values of the flake diameter and aspect ratio of mica are 1.8 and 4.6 μm, respectively. The heat-treatment temperature of critical point locates at 1060 °C. When $T_C \leqslant 1060$ °C, the bending strength increases with the increase of heat-treatment temperature ascribing to the randomly oriented and interlocked mica crystals, which cause crack divert or blunt to limit the further development of the flaw size and increase the surface energy of fracture. While $T_C > 1060$ °C, the increased boundary shear stress arising from the mismatch of thermal coefficient between the mica crystals and the residual glass phase results in the decrease of strength.

Acknowledgement

The authors are grateful to Professor Hui Gu for many helpful discussions and comments.

References

1. Grossman, D. G., Machinable glass-ceramics based on tetrasilicic mica. *J. Am. Ceram. Soc.*, 1972, **55**, 446–449.
2. Chyung, C. K., Beall, G. H. and Grossman, D. G., Microstructure & mechanical properties of mica glass-ceramics. In *Proceeding of 5th International Materials Symposium*. University of California Press, Berkeley, CA., 1971, pp. 1167–1194.
3. Daniels, W. H. and Moore, R. E., Crystallization of a tetrasillicic fluormica glass. *J. Am. Ceram. Soc.*, 1975, **58**, 217–221.
4. Dennis, Mog., Machinable glass-ceramics: a new material for vacuum equipment. *Vacuum*, 1975, **26**(1), 25–29.
5. Li, L. and Yu, H., Reseach on bioctive glass-ceramics. *J. Non-Cryst. Solids*, 1989, **112**, 156–160.
6. Saraswati, V., Additive induced crystallization of mica phase in $K_2O\text{–}SiO_2\text{–}MgO\text{–}F$ glass-ceramics. *J. Non-Cryst. Solids*, 1990, **124**, 254–257.
7. Chyung, C. K., Beall, G. H. and Grossman, D. G., Fluorophlogopite mica glass-ceramics. *10th Intern Congress On Glass (Tokyo), 14, 1974, 33–40*.
8. Höland, W. and Vogel, W., A new type of phlogopite crystal in machinable glass-ceramics. *Glass Technolgy*, 1983, **24**(6), 318–322.
9. Hidero, U., Koh, M. and Kohei, K., Improvement of mechanical properties of machinable glass ceramics through postmaching heat treatments. *J. Am Ceram. Soc.*, 1992, **75**(8), 2300–2301.

10. Reise, M., Berger, A. and Muller, G., Transformation toughening of machinable mica glass ceramics. *Proc. Of X.V.II. Inter. Cong. On Glass, Beijing: Chinese Ceram. Soc*., 1995, **5**, 241–246.
11. Dong, S. B., Kwang, S. N. and John, S. C., Mechanical properties of mica glass-ceramics. *J. Am. Ceram. Soc*., 1995, **78**(5), 1217–1222.
12. Tomoko, U., Toshihiro, K. and Kiichi, N., High strength mica-containing glass-ceramics. *J. Am. Ceram. Soc*., 1991, **74**(12), 3139–3141.
13. Beall, G. H. and Chain silicate glass ceramics, J., Non-Cryst. *Solids*, 1991, **129**, 163–173.
14. Tomoko, U. and Toshihiro, K., Mechanical properties of barium-mica containing glass ceramics. *J. Soc. Ceram. Jpn*., 1992, **100**(3), 15–319.
15. Tomoko, U., Toshihiro, K., Shin, N. and Akira, J. I., Microstucture of mica-based nanocomposite glass-ceramics. *J. Am. Ceram. Soc*., 1993, **76**(2), 539–541.
16. Huang, W. and Zhu, P., Change in microstructure during the crystallization process of lepidolite based glass-ceramics. *Journal Of The Chinese Silicate Society*, 1983, **11**(4), 430–434.
17. Zhu, P., The applications of machinable glass-ceramics in instrument industry. *Journal of The Chinese Instrument Materials*, 1981, **12**(1), 20–24.